Optical Engineering 47(4), 044402 (April 2008)

Sensitivity dependence with respect to diaphragm thickness in guided-wave optical pressure sensor based on elasto-optic effect

Hiroyuki Nikkuni, MEMBER SPIE
Yu Watanabe
Niigata University
Graduate School of Science and Technology
8050 Ikarashi 2-no-cho
Nishi-ku, Niigata 950-2181, Japan

Masashi Ohkawa, MEMBER SPIE
Takashi Sato, MEMBER SPIE
Niigata University
Faculty of Engineering
8050 Ikarashi 2-no-cho
Nishi-ku, Niigata 950-2181, Japan

Abstract. We experimentally investigated the relationship between sensitivity and diaphragm thickness in a glass-based guided-wave optical pressure sensor using intermodal interference between the fundamental TM-like and TE-like modes. The sensor consists of a rectangular diaphragm and a straight single-mode waveguide on the diaphragm. The sensitivity is theoretically known to be inversely proportional to the square of the diaphragm thickness. In this study, to examine this relationship, four sensors with diaphragm thicknesses of 0.30 mm, 0.22 mm, 0.20 mm, and 0.15 mm were fabricated. The area of the diaphragm was 10 mm × 10 mm. For the waveguide position nearest to the center of the diaphragm, the measured sensitivities almost agreed with the theoretical ones.
[DOI: 10.1117/1.2909669]

Subject terms: guided-wave optics; pressure sensor; diaphragm; glass waveguide; elasto-optic effect.

Paper 070773R received Sep. 14, 2007; revised manuscript received Nov. 24, 2007; accepted for publication Dec. 30, 2007; published online Apr. 25, 2008.

1 Introduction

Micro-opto-mechanical devices have increasingly attracted attention due to the remarkable developments in micromachining technology in recent years.[1,2] A guided-wave optical pressure sensor using a micro-machined diaphragm is one such promising micro-opto-mechanical device. Several groups have demonstrated guided-wave optical pressure sensors with diaphragms since the late 1980s.[3–8] Our group has been developing silicon-based and glass-based guided-wave optical pressure sensors using intermodal interference between the fundamental TM-like and TE-like modes.[7–9] The sensitivities of these pressure sensors based on the elasto-optic effect, including our sensors, are theoretically known to be inversely proportional to the square of the diaphragm thickness.[10] The relationship between sensitivity and diaphragm thickness is very significant in designing the sensors with higher sensitivity, but has not yet been experimentally confirmed. In this study, the relationship was experimentally examined using four glass-based guided-wave optical pressure sensors, which had the same diaphragm dimensions but with differing thicknesses. The sensitivity also depends on the position of the sensing waveguide.[8,9] To reduce errors due to misalignment of the sensing waveguide to a minimum, a sufficient number of waveguides were formed, closely spaced on the diaphragm. The measured sensitivities of the four sensors were in fairly good agreement with the theoretical ones, especially in the waveguide position around the center of the diaphragm. Incidentally, a glass substrate was utilized to build the sensor in this study although silicon is a more familiar substrate for sensors incorporated with mechanical structures. The use of a glass substrate provides a reliable comparison between the theoretical and experimental results since its mechanical and optical properties are well known. If silicon is used as a substrate, the theoretical calculation becomes rather complicated because a diaphragm usually consists of several layers. Moreover, the physical properties of all layers may not be always known exactly. Thus, it would not be easy to ensure reliability in a quantitative comparison with silicon used. Even if the experiments are done not using silicon substrate but using glass substrates, the results can be applied to the more familiar silicon-based guided-wave optical pressure sensors although proper modifications might be required in some cases.

2 Principle of Sensor Operation

Figure 1 shows a glass-based guided-wave optical pressure sensor using intermodal interference. The sensor consists of a rectangular diaphragm as a pressure-sensitive mechanical structure and a single-mode waveguide across the diaphragm. The sensor is placed between a pair of crossed polarizers. The polarization of the input polarizer is oriented at 45° with respect to the sensor surface. The light beam through the input polarizer is coupled to the fundamental TM-like and TE-like modes at equal intensities. When a pressure difference is applied to the diaphragm, the diaphragm is distorted. The distortion causes strain, which induces a change in the refractive index of the diaphragm by the elasto-optic effect. The index change yields phase retardation in the guided light, which is propagated in the waveguide across the diaphragm. Since the phase retardation is dependent on the guided modes, the phase difference between the fundamental TM-like and TE-like modes varies as a function of the applied pressure difference. The lightwave has linear, elliptic, or circular polarization at the

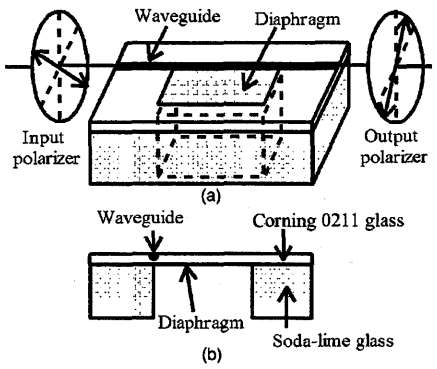

Fig. 1 (a) Schematic drawing of the glass-based guided-wave optical pressure sensor placed between a pair of crossed polarizers and (b) its cross-sectional view.

end of the waveguide, corresponding to the induced phase difference between the two guided modes. The crossed output polarizer converts the polarization-modulated light into intensity-modulated light. The intensity of the light beam passing through the output polarizer sinusoidally changes with the applied pressure. Therefore, the applied pressure can be determined from the output intensity.

3 Theoretical Results

In this study, the phase sensitivity, defined as the resultant phase difference per unit pressure, is used as the sensor sensitivity. In the theoretical analysis, the phase sensitivity dependence with respect to diaphragm thickness was derived, following the mathematical description in Ref. 9. The normal stress on the surface of the diaphragm largely contributes to the phase retardation and is inversely proportional to the square of the diaphragm thickness. Assuming that the relationship between stress and the index change is linear, phase retardation due to the anisotropic index change is inversely proportional to the square of the diaphragm thickness. Therefore, the phase sensitivity is in inverse proportion to the square thickness. Figure 2 shows the calculated phase sensitivity as a function of diaphragm thickness when the side lengths of the diaphragm remain constant. It was assumed that the pressure was uniformly applied over the diaphragm, and all sides of the diaphragm

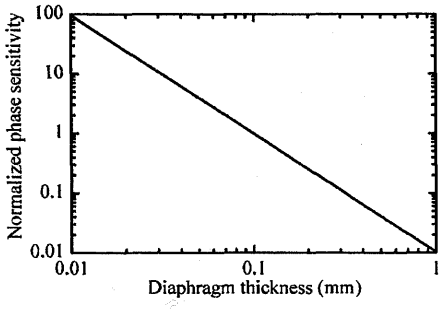

Fig. 2 Phase sensitivity as a function of diaphragm thickness. The phase sensitivity is normalized to be at unity at 0.1 mm thick.

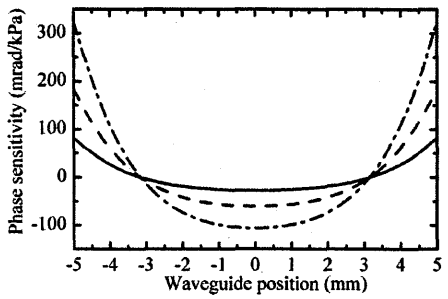

Fig. 3 Relationships between phase sensitivity and waveguide position. Solid, broken, and dash-dot lines represent the calculated results for 0.30 mm, 0.20 mm, and 0.15 mm thick, respectively. Diaphragm area was set to be 10 mm × 10 mm in the calculation.

are rigidly clamped. The wavelength of the guided light was set at 633 nm. In the figure, the sensitivity is normalized to be at unity at 0.1 mm thick. Since the sensitivity is inversely proportional to the square of the diaphragm thickness, the slope of the curve is −2 in the log-log graph.

Incidentally, sensitivity is also dependent on the waveguide position. This dependence is undesirable in this study since it may cause sensitivity deviation due to misalignment of the sensing waveguide. Figure 3 shows the relationships between calculated sensitivity and waveguide position. In the calculation, the area of the diaphragm was set to be 10 mm × 10 mm, and thicknesses of 0.30 mm, 0.20 mm, and 0.15 mm were chosen. The diaphragm material was assumed to be Corning 0211 glass, of which the diaphragms of the fabricated sensors in this study were made. In the figure, the waveguide positions of ±5 mm correspond to the edge of the diaphragm, whereas a position of 0 mm corresponds to the center of the diaphragm. At the edge, the sensitivity is at a maximum but is significantly affected by any deviation of the waveguide away from the edge. At the center, the misalignment tolerance of the waveguide position is excellent although the sensitivity is 33% of that at the edge of the square diaphragm. Comparing sensitivity, the waveguide position at the center is much better than that at the edge.

4 Experiments

4.1 *Fabrication*

We made four sensors out of two glass substrates: a Corning 0211 glass as a diaphragm plate and a soda-lime glass with a square hole as a support structure of the diaphragm. The diaphragm thicknesses of the four sensors were 0.30 mm (sensor 1), 0.22 mm (sensor 2), 0.20 mm (sensor 3), and 0.15 mm (sensor 4). The diaphragm areas of all sensors were 10 mm × 10 mm. These sensors had 22 straight waveguides, spaced at 0.5-mm intervals, to assess the dependence of the sensitivity on the waveguide position on the diaphragm.

In fabrication, a thin aluminum film was first evaporated on a Corning 0211 glass substrate. On the aluminum film, the waveguide patterns with a width of about 5 μm were engraved by a photolithographic process. Then the glass was immersed in pure KNO_3 for 2 h at 400 °C using the patterned aluminum film as a mask to make single-mode

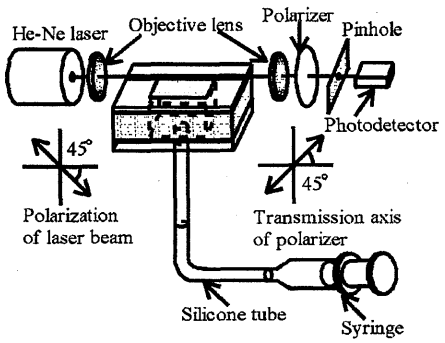

Fig. 4 Experimental setup used to measure the output intensity versus the applied pressure.

channel waveguides. Before two substrates were put together, one of the waveguides was aligned along a side of the hole in the soda-lime glass. Finally, both substrates were bonded together by UV adhesion.

4.2 *Experimental Results and Discussions*

Figure 4 illustrates the experimental setup to measure the output intensity versus the applied pressure. The fabricated sensors were tested using a linearly polarized He-Ne laser at 633 nm. The polarization of the laser beam was set at 45° to the sensor surface, so that the input polarizer, shown in Fig. 1, was not utilized in this experiment. Pressure was applied to the diaphragm by connecting a syringe to the sensor with a silicone tube. The pressure difference, ranging from −25 kPa to 30 kPa at least, was applied to the diaphragm by pulling and pushing the plunger of the syringe and was determined from the ideal gas law. A positive value of the pressure represents that the pressure under the diaphragm is higher than the atmospheric pressure. Moreover, the output light from the sensor was passed through a pinhole to block stray light. Output power was detected by a photodetector.

Figures 5(a)–5(d) show the experimental results for the waveguide nearest the center of the diaphragm in sensors 1–4, respectively. Filled squares in each figure represent the experimental data, and the solid line shows a computer projection of the experimental data. A half-period of the output intensity is called the halfwave pressure, which corresponds to the phase difference of π rad. From the obtained halfwave pressure, the phase sensitivity can be calculated. From Figs. 5(a)–5(d), the halfwave pressure are evaluated to be 117 kPa, 61 kPa, 53 kPa, and 30 kPa, and the corresponding phase sensitivities are 27 mrad/kPa, 52 mrad/kPa, 59 mrad/kPa, and 105 mrad/kPa, respectively. Table 1 indicates the calculated and measured sensitivities for the waveguide nearest the center of the diaphragm. Also, Fig. 6 shows the calculated and measured sensitivities as a function of the diaphragm thickness. It is found from Table 1 and Fig. 6 that the measured sensitivities of the four sensors almost agree with the theoretical ones. This result is rather reliable since the misalignment tolerance of the waveguide position is excellent around the center, as described in Section 3. The same measurements were also taken for the other waveguides of the four fabricated sensors. Figure 7 indicates the measured sensitivity versus the waveguide position in the three sensors. No results of sensor 2 are shown in Fig. 7, since the measured sensitivities of sensor 2 are very similar to those of sensor 3. The solid, broken, and dash-dot lines represent the calculated sensitivities as shown in Fig. 3. The minus sign was given to the measured sensitivities near the center of the

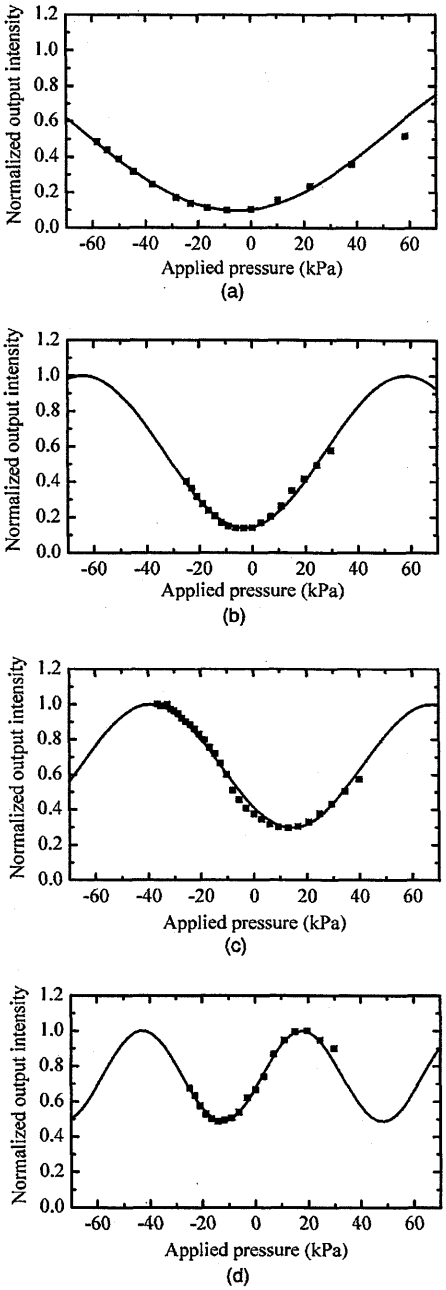

Fig. 5 Experimental results of normalized output intensity versus applied pressure for the waveguide nearest to the center of the diaphragm. Figures (a)–(d) are for sensors 1–4, respectively.

Table 1 The calculated and measured sensitivities for the waveguide nearest the center of the diaphragm of sensors 1–4.

Sensor #	Diaphragm Dimensions (mm × mm × mm)	Calculated Sensitivity (mrad/kPa)	Measured Sensitivity (mrad/kPa)
1	10×10×0.30	27	27
2	10×10×0.22	50	52
3	10×10×0.20	60	59
4	10×10×0.15	107	105

diaphragm according to the theoretical results although the sign is not distinguishable in this measurement. In Fig. 7, the measured sensitivities of the three sensors almost agree with the theoretical sensitivities at any position around the center of the diaphragm. Incidentally, for the waveguide near the edge, the measured sensitivities are lower than the calculated sensitivities. Such a difference is attributed to a relaxation of induced strain near the diaphragm edge. The relaxation is caused by imperfect bonding by UV adhesion, which reduced the rigidity of the support structure surrounding the diaphragm. The imperfect bonding does not, however, greatly affect the sensitivities around the center. Additionally, since the problem of imperfect bonding comes from the sensor structure, it is unnecessary to be considered in the more familiar silicon-based sensors. From the above discussions, it can be concluded that the sensitivity is inversely proportional to the square of the diaphragm thickness.

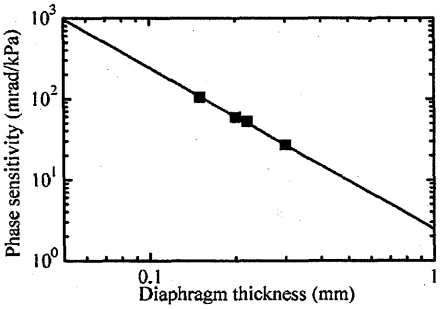

Fig. 6 Measured sensitivities for the waveguide nearest to the center of the diaphragm of sensors 1–4 are shown as filled squares. The solid line indicates the calculated sensitivities as a function of diaphragm thickness.

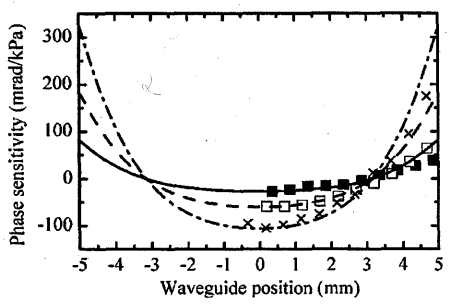

Fig. 7 Measured sensitivity as a function of the waveguide position on the diaphragm. ■, □, and × represent the measured sensitivities of sensors 1, 3, and 4, respectively. Also, solid, broken, and dash-dot lines represent the calculated sensitivities of sensors 1, 3, and 4, respectively.

Incidentally, in Figs. 5(a) and 5(b), the sensor cannot distinguish positive pressure from negative pressure. To measure both positive pressure and negative pressure, the initial phase difference should ideally be set at $\pi/2$ rad. In the sensor using the intermodal interference, the initial phase difference can be controlled by adjustment of the waveguide length if the effective indices of the TM-like and TE-like modes are different. However, since the effective index difference of the single-mode ion-exchanged glass waveguide is small, the waveguide length of the sensor becomes long to produce the initial phase difference of $\pi/2$ rad. Then, such an adjustment is not practical, because the sensor size becomes large. In practical applications, the imbalanced Mach–Zehnder interferometer is appropriate rather than the intermodal interferometer since the sensor size can be smaller. In the imbalanced Mach–Zehnder interferometer, the initial phase difference can be adjusted by introducing a path-length difference of the sensing and reference waveguides.

5 Conclusions

The relationship between sensitivity and diaphragm thickness was experimentally examined using four fabricated sensors with different diaphragm thicknesses. In the experimental results, for the waveguide nearest the center of the diaphragm, the measured sensitivities of the four sensors almost agree with the theoretical sensitivities. The measured relationship is highly reliable because the measured sensitivities also agree with the theoretical ones in several waveguide positions around the center and similar results were obtained for other sensors with the same dimensions of the diaphragms. By thinning the diaphragm, a highly sensitive sensor can be realized while maintaining a diaphragm that is sufficiently resistant to pressure.

Acknowledgments

This work is supported in part by a Grant-in-Aid for Scientific Research (No. 17360157) from the Japan Society for the Promotion of Science.

References

1. M. Tabib-Azar and G. Beheim, "Modern trends in microstructures and integrated optics for communication, sensing, and actuation," *Opt. Eng.* **36**(5), 1307–1318 (1997).
2. P. Rai-Choudhury, Editor, *MEMS and MOEMS Technology and Applications*, SPIE Press, Ballinghan, WA (2000).
3. M. Ohkawa, M. Izutsu, and T. Sueta, "Integrated optic pressure sensor on silicon substrate," *Appl. Opt.* **28**(23), 5153–5157 (1989).
4. G. N. De Brabander, J. T. Boyd, and G. Beheim, "Integrated optical ring resonator with micromechanical diaphragm for pressure sensing," *IEEE Photonics Technol. Lett.* **6**, 671–673 (1994).
5. G. N. De Brabander, G. Beheim, and J. T. Boyd, "Integrated optical micromachined pressure sensor with spectrally encoded output and temperature compensation," *Appl. Opt.* **37**, 3264–3267 (1998).
6. H. Porte, V. Gorel, S. Kiryenko, J. Goedgebuer, W. Daniau, and P. Blind, "Imbalanced Mach–Zehnder interferometer integrated in micromachined silicon substrate for pressure sensor," *J. Lightwave Technol.* **17**, 229–233 (1999).
7. T. Goto, A. Yamada, M. Ohkawa, S. Sekine, and T. Sato, "An experi-

mental investigation of sensitivity dependence with respect to waveguide position on a micromachined diaphragm in a silicon-based integrated optic pressure sensor," *Proc. SPIE* **4591**, 337–344 (2001).
8. M. Ohkawa, Y. Shirai, T. Goto, S. Sekine, and T. Sato, "Silicon-based integrated optic pressure sensor using intermodal Interference between TM-like and TE-like modes," *Fiber Integr. Opt.* **21**, 105–113 (2002).
9. M. Ohkawa, K. Hasebe, S. Sekine, and T. Sato, "Relationship between sensitivity and waveguide position on the diaphragm in integrated optic pressure sensors based on the elasto-optic effect," *Appl. Opt.* **41**(24), 5016–5021 (2002).
10. M. Ohkawa, T. Abe, S. Sekine, and T. Sato, "Integrated optic micropressure sensor using ring resonator," *Electron. Commun. Jpn., Part 2: Electron.* **79**, 1–10 (1996).

Hiroyuki Nikkuni received his BE and ME degrees from Niigata University, Japan, in 2004 and 2006, respectively. He is currently pursuing his DEng degree. His research interests include silicon-based and glass-based guided-wave optical pressure sensors and microphones.

Yu Watanabe received his BE degree from Niigata University, Japan, in 2007. He is pursuing his ME degree. His research interests are glass-based guided-wave optical pressure sensors and microphones.

Masashi Ohkawa received his BE, ME, and DEng degrees in electrical engineering from Osaka University, Japan, in 1984, 1986, and 1989, respectively. In 1989, he joined the Faculty of Engineering at Niigata University as a research associate, where he is currently professor. His research interests include integrated optic devices and holography.

Takashi Sato received his BS, MS, and PhD degrees in electronic engineering from Kyoto University in Japan 1976, 1978, and 1983, respectively. He is currently a professor at Niigata University. His research subjects are in the laser production of alkali hydride particles, the frequency stabilization of dye lasers and semiconductor lasers, the oscillation frequency shift of a semiconductor laser in a magnetic field, and the application of nonlinear optical effects for frequency stabilization of a semiconductor laser.